International Journal of Mass Spectrometry 305 (2011) 58–68

Contents lists available at ScienceDirect

International Journal of Mass Spectrometry

journal homepage: www.elsevier.com/locate/ijms

Novel concept for the mass spectrometric determination of absolute isotopic abundances with improved measurement uncertainty: Part 3—Molar mass of silicon highly enriched in ^{28}Si

Axel Pramann[a,*], Olaf Rienitz[a], Detlef Schiel[a], Bernd Güttler[a], Staf Valkiers[b]

[a] Physikalisch-Technische Bundesanstalt (PTB), Bundesallee 100, 38116 Braunschweig, Germany
[b] Institute for Reference Materials and Measurements (EC-JRC-IRMM), Retieseweg 111, 2440 Geel, Belgium

ARTICLE INFO

Article history:
Received 17 January 2011
Received in revised form 26 May 2011
Accepted 26 May 2011
Available online 12 June 2011

Keywords:
Molar mass
Silicon
MC-ICP-MS
Isotope dilution mass spectrometry
Measurement uncertainty
Avogadro constant

ABSTRACT

A novel method of isotope amount ratio measurements using state-of-the-art techniques of a double focusing sector field mass spectrometer combined with isotope dilution mass spectrometry (IDMS) has been applied connecting analytical chemistry with metrology in chemistry aiming at the determination of the Avogadro constant (N_A). The molar mass M("Si28") and the corresponding isotopic composition of an artificial silicon crystal material highly enriched in the ^{28}Si isotope has been measured for the first time using a combination of a modified IDMS- and a multicollector-ICP-mass spectrometer (MC-ICP-MS) technique. A value M("Si28") = 27.97697027(23) g/mol has been determined. This corresponds to a relative uncertainty $u_{rel} = 8.2 \times 10^{-9}$ ($k = 1$). From this silicon crystal material two 1 kg spheres were manufactured which are used by the International Avogadro Coordination (IAC) in order to reassess (N_A) with an associated relative measurement uncertainty $u_{rel}(N_A) \leq 1 \times 10^{-8}$. The experiment presented here is the advancement and completion of parts 1 and 2 of this series of papers, describing the theoretical and general experimental applicability of the novel method. The current work summarizes the experimental findings aiming at the determination of the molar mass of the "Si28" material with the lowest uncertainty possible so far. The experimental prerequisites and bottlenecks for examining this highly enriched silicon material as well as experimental proofs for the verification of the presented results are described in detail. The experimental results are supplemented by an uncertainty budget according to the Guide to the Expression of Uncertainty in Measurement (GUM).

1. Introduction

The current paper bridges a gap between novel state-of-the-art mass spectrometric methods in analytical chemistry and metrology using magnetic sector field mass spectrometry—in particular high resolution inductively coupled plasma mass spectrometry. It shows that the use of a high resolution multicollector-ICP-MS instrument reduces the measurement uncertainty compared to experiments using gas phase mass spectrometers [1]. The respective advantages such as simultaneous isotope amount ratio measurement and quasi-simultaneous blank quantification as well as exact calibration during the measurement are presented. In the context of the redefinition of the SI unit kilogram, the more exact knowledge and thus new determination of fundamental constants like the Avogadro constant N_A with further reduced measurement uncertainty is a main prerequisite. Besides the Watt balance experiments, the International Avogadro Coordination (IAC) conducts a parallel route for the determination of N_A with the intention to achieve $u_{rel}(N_A) \leq 1 \times 10^{-8}$. The general principle of this project is based on the hypothetical counting of atoms in an almost perfect crystal sphere made of 1 kg of silicon. This is called the "XRCDMM" method [2–6]. In the past the limiting uncertainty was described by the molar mass of natural silicon [5]. Intense work to overcome this problem led to a sub-project of the IAC devoted to the manufacturing of an ultra-pure silicon single crystal with an enrichment in ^{28}Si higher than 99.99%. In the following, this material is denoted briefly as "Si28". Using this material, the molar mass has to be determined with a relative uncertainty of at least $u_{rel}(M) \leq 1 \times 10^{-8}$, sufficient for the reassessment of N_A on the same level of uncertainty: $u_{rel}(N_A) \leq 1 \times 10^{-8}$. For this reason the measurement of the molar mass of "Si28" is a great challenge and one of the key experiments for the measurement of N_A. At this stage of the project, two silicon spheres (AVO28-S5 and AVO28-S8) cut from the original

Abbreviations: IDMS, isotope dilution mass spectrometry; IAC, International Avogadro Coordination; VE, virtual element; GUM, Guide to the Expression of Uncertainty in Measurement; MC-ICP-MS, multicollector inductively coupled plasma mass spectrometer; "Si28", silicon material highly enriched with respect to ^{28}Si; "Si29", silicon material highly enriched with respect to ^{29}Si; "Si30", silicon material highly enriched with respect to ^{30}Si; XRCDMM, X-ray crystal density molar mass.

* Corresponding author. Tel.: +49 531 592 3219; fax: +49 531 592 3015.
E-mail address: Axel.Pramann@ptb.de (A. Pramann).

1387-3806/$ – see front matter © 2011 Elsevier B.V. All rights reserved.
doi:10.1016/j.ijms.2011.05.017

float-zone ingot, artificially highly enriched with the ^{28}Si isotope ($x(^{28}\mathrm{Si}) > 0.9999$ mol/mol) are the objects under investigation by the IAC.

The aim of the current work is to determine the isotopic abundances, and thus the molar mass of the "Si28" material, with a relative uncertainty of $u_{\mathrm{rel}}(M(\text{"Si28"})) \leq 1 \times 10^{-8}$. This was done as described in parts 1 and 2 of this series by the combination of several advantageous techniques, like the simultaneous mass spectrometric detection of ion currents and thus isotope amount ratios (static mode) with reduced uncertainty (MC-ICP-MS) [7,8]. Another main benefit of the applied technique is the ability for the correction of the contamination with (mainly natural) silicon by measuring the blank (solvent plus instrumental background) during the experiment. It is crucial to avoid a contamination of "Si28" with natural silicon during the entire experiment. For this reason the transfer of the crystal into the liquid sample is done quantitatively in one single step by using aqueous NaOH avoiding cumulative contaminations. The determination of the molar mass is completed by applying a modified IDMS technique—which is described in part 1 [7]. It makes use of a so-called *virtual element* (VE)—consisting of the minor abundant silicon isotopes ^{29}Si and ^{30}Si in their matrix, namely the sum of all three Si isotopes (^{28}Si, ^{29}Si, ^{30}Si). Moreover, a new analytical and non-iterative determination of calibration factors (K) for the correction of isotope amount ratios was applied [9]. In order to obtain an estimation of the homogeneity of the "Si28" crystal with respect to the isotopic composition, several samples were measured along the axis of the original ingot which was divided into parts numbered from 1 to 11. The two spheres used for volume, surface, density and mass determinations originate from parts 5 and 8. Molar mass experiments were performed using crystal samples of these areas, as well as from parts 4 and 9. Verification experiments concerning the correctness of the mass spectrometric measurements, like the investigation of molecular interferences, dependence of total silicon and matrix concentration, influence of signal tailing, and drift of the mass scale, were performed to underline the reliability of the results. Finally, the results of this work have broader applications for other isotope systems (e. g. magnesium).

2. Principle of the molar mass determination

The basic interrelations of the novel theoretical principle and derivation for the determination of the molar mass are described in detail in [7]. The core idea of the novel method makes use of a modified IDMS technique. To guide the reader, only a brief overview is given here. Generally, the application of IDMS guarantees most precise results in determining mass fractions w of analytes in their matrix [10–16]. However, the modified IDMS technique applied in this work concentrates on the determination of the mass fraction w_{imp} of the VE (^{29}Si and ^{30}Si), which consists of the less abundant isotopes in the sample matrix (^{28}Si, ^{29}Si, and ^{30}Si). The determination of the isotope amount ratio (R_{x}) and the mass fraction w_{imp} of the VE will mainly lead to the molar mass M("Si28"). A prerequisite is the knowledge of the molar masses of the isotopes $M(^{28}\mathrm{Si})$, $M(^{29}\mathrm{Si})$, and $M(^{30}\mathrm{Si})$. These are given in the current IUPAC reference tables [17]. It must be noted that these values were revised in [18], but are not yet used in metrology in chemistry as reference values. The new data give the same numerical results in M("Si28"), but with slightly smaller associated measurement uncertainties. For the sake of a conservative uncertainty budget, the molar mass data of ^{28}Si, ^{29}Si, and ^{30}Si were, therefore, taken from [17].

The molar mass of the "Si28" sample is

$$M(\mathrm{Si}) = \sum_{i=28}^{30} [x_{\mathrm{x}}(^{i}\mathrm{Si}) \times M(^{i}\mathrm{Si})] \tag{1}$$

$$\vdots$$

$$M(\mathrm{Si}) = \frac{M(^{28}\mathrm{Si})}{1 + (m_{\mathrm{yx}}/m_{\mathrm{x}})(M(^{28}\mathrm{Si})(1+R_{\mathrm{x}}) - M(^{29}\mathrm{Si}) - R_{\mathrm{x}}M(^{30}\mathrm{Si}))/(R_{\mathrm{y},28}M(^{28}\mathrm{Si}) + M(^{29}\mathrm{Si}) + R_{\mathrm{y}}M(^{30}\mathrm{Si}))((R_{\mathrm{y}} - R_{\mathrm{bx}})/(R_{\mathrm{bx}} - R_{\mathrm{x}}))} \tag{2}$$

with the amount-of-substance fractions $x_{\mathrm{x}}(^{28}\mathrm{Si})$, $x_{\mathrm{x}}(^{29}\mathrm{Si})$, and $x_{\mathrm{x}}(^{30}\mathrm{Si})$. In order to avoid numerical deviations in the last digits due to rounding errors, a comprehensive expression has been derived for the molar mass as a function of the measured isotope amount ratios R and masses m, avoiding the implementation of intermediate results. These formulae (Eqs. (2) and (18), respectively) and their derivations are given in Appendix A. The quantities are defined in [7]. The novel concept using a modified IDMS technique [7] has recently been independently checked and validated by INRIM (Istituto Nazionale di Ricerca Metrologica; Italy) [19]. Isotope amount ratio analyses by ICP-MS are affected by instrumental mass discrimination/bias [20–22]. Thus, a correction of the measured isotope amount ratios by calibration factors K is obligatory [7]. In this context, a new analytical method for the direct and exact measurement and calculation of these calibration factors has been developed [9], which was applied also in this study. Fig. 1 (top) displays the principle of the K factor evaluation, whereas Fig. 1 (bottom) shows the relations between the isotope amount ratios and masses which have to be measured, the K factors, and finally the derived molar mass M. Quantities were described in detail in [7] and [8].

3. Experiment

The experimental details of the mass spectrometric determination of the isotopic abundances of "Si28" are described mainly in detail in [8]. Here, only a brief description is given. Additional important and differing experimental details in the case of studying "Si28" are presented in more detail.

3.1. Instrumentation

Isotope amount ratio measurements were conducted using a Thermo Finnigan Neptune MC-ICP-MS [23,24]. The main instrumental parameters are listed in Table 1 of [8]. The Faraday cup L3 was not used (moved aside) during the measurement of "Si28". A standard high performance nickel skimmer cone was used. The mean sensitivities were: (1.0 ± 0.1) V/(μg/g) for ^{28}Si (MR, natural silicon) and (0.5 ± 0.1) V/(μg/g) for ^{28}Si (HR, natural silicon). The resolutions applied were: 6000 (MR, K-factor measurement) and 8000 (HR, "Si28" measurement). In order to determine the molar mass of "Si28", it is important to avoid any contamination with silicon. Otherwise, the isotope ratio $R(^{30}\mathrm{Si}/^{29}\mathrm{Si})$ of the original sample will be strongly biased. Therefore, special equipment, like a custom-made sapphire torch with a boron nitride shield (AHF analysentechnik AG, Germany), was used instead of a quartz torch. Also, the spray chamber as well as the tubings were made of PFA/PTFE material, almost Si-free and inert. The aerosols were generated using a PFA 50 type nebulizer (Elemental Scientific Inc., 50 μL min^{-1} flow rate). An experimental run consisted of the measurement of the "Si28" samples and respective IDMS blends included in a first sequence (A) followed by the second sequence (B), where the calibration factors were measured using natural silicon. This separation is necessary, because when measuring the "Si28" material ($w(\mathrm{Si}) = 4000$ μg/g), the high silicon

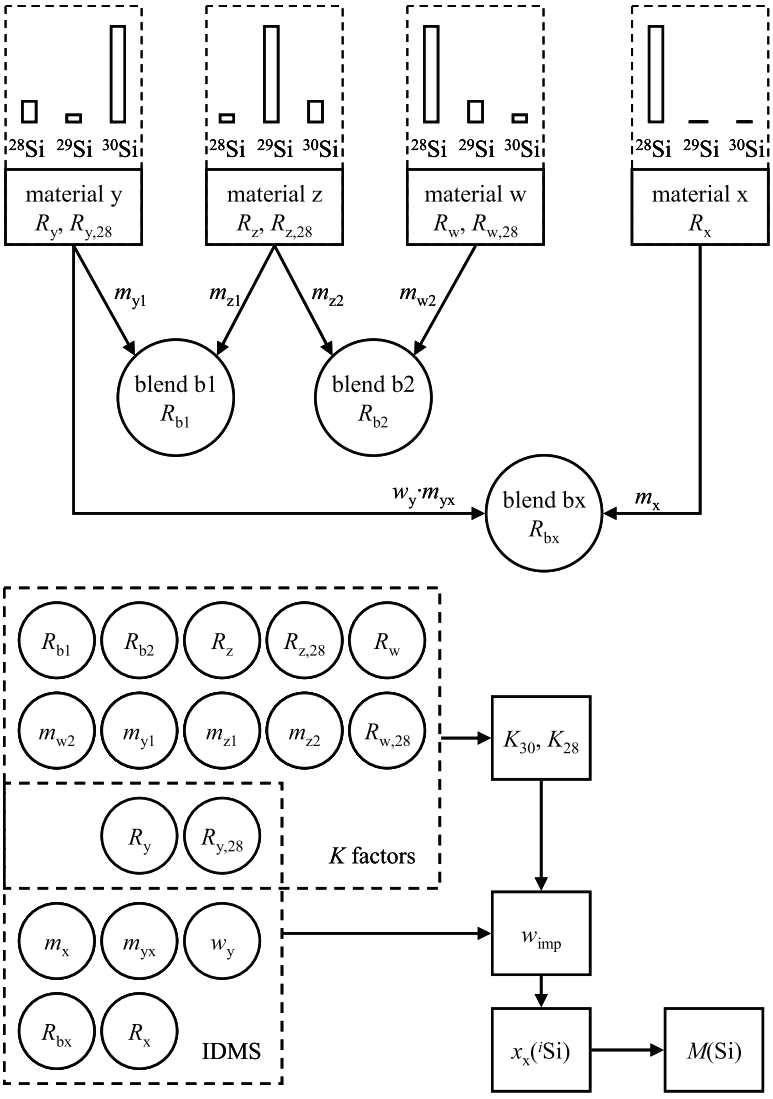

Fig. 1. Top: preparation of the IDMS blend bx and blends b1 and b2, which are used for the determination of the calibration factors *K*. Altogether, ten isotope amount ratios *R* as well as six masses *m* are necessary to calculate the molar mass according to Eq. (1). Bottom: relation between isotope amount ratios *R* and masses *m* for *K* factor determination, modified IDMS and the resulting amount-of-substance and molar mass determination.

concentration and the extreme enrichment in ^{28}Si might damage the Faraday cup L3. For this reason, in sequence (A) only the cups C (^{29}Si) and H3 (^{30}Si) were used and the L3 cup (^{28}Si) was moved aside, so the $^{28}Si^{+}$ beam cannot hit the detector. After sequence (A), the cup configuration was changed (for using all three: L3, C, and H3) for the measurement of the calibration factors using natural silicon (WASO17). Sequence (A) was executed in the high resolution mode ($M/\Delta M = 8000$), whereas sequence (B) was performed in medium resolution mode ($M/\Delta M = 6000$) in order to benefit from higher transmission. However, sequences (A) and (B) were treated as a "single run", because the plasma was kept running between (A) and (B) and most experimental parameters were identical in order to be allowed to apply the calibration factors measured in (B) to (A). Verification experiments – described later – were performed to assure this precondition. In Section 3.3, more details about the sequences and data aquisiton parameters were provided.

3.2. Materials and reagents

A Millipore water purification system (ELIX 5 UV, Milli-Q Element A10, Millipore Corporation, USA) was used to provide the ultrapure water used in this study ($\sigma \geq 18\,\Omega$ cm). It is worth to note that all bottles and vials or other equipment (all made of PFA) which came in contact with the samples or solutions had been carefully cleaned beforehand via several steps [8]. Silicon "Si28" sample crystals were slices of approximately 380–420 mg each, cut from the surrounding offcut material of the "Si28" spheres of the original float-zone (FZ) ingot. Samples mainly from parts 5 and 8 were investigated. The original location of each sample can be traced back and homogeneity studies are still under way. For the IDMS blend a spike material—a silicon single crystal highly enriched in ^{30}Si ("Si30") was used. This has been prepared like the other two materials (natural silicon, namely WASO17 and "Si29") from slices of approximately 50–70 mg each, cut from the respective float-

zone crystal. The chemical purity of the crystals has been tested by infrared spectroscopy and the chemicals used were of the highest purity commercially available [8]. Sample and solution preparation was performed gravimetrically (air buoyancy correction). After cleaning and etching, the silicon samples were initially weighed by the PTB mass laboratory. The weighed sample crystals were then dissolved in aqueous sodium hydroxide (Merck Suprapur 99.99%, $w(\mathrm{NaOH}) = 0.17$ g/g) in order to yield stock solutions according to

$$\mathrm{Si} + 4\,\mathrm{OH}^- \rightarrow \mathrm{SiO_4^{4-}} + 2\,\mathrm{H_2} \quad (3)$$

In the case of the "Si28" material, the stock solutions have concentrations in the range of $w(\mathrm{Si}) = 4000$ μg/g in an aqueous matrix containing $w(\mathrm{NaOH}) = 0.001$ g/g. These solutions were directly used for the measurement in the MC-ICP-MS. About half of the respective "Si28" stock solution was used to prepare the IDMS blend together with "Si30" solutions ($w(\mathrm{Si}) = 1$ μg/g; $w(\mathrm{NaOH}) = 0.001$ g/g) and aqueous NaOH ($w(\mathrm{NaOH}) = 0.001$ g/g). The silicon material solutions (natural silicon, namely WASO17, "Si29" and "Si30") were prepared as desribed in [8] (final concentrations: $w(\mathrm{Si}) = 4$ μg/g in $w(\mathrm{NaOH}) = 0.0001$ g/g). Blank solutions for the bracketing measurements had the following concentrations: $w(\mathrm{NaOH}) = 0.001$ g/g in the case of the "Si28" measurements (sequence (A)) and $w(\mathrm{NaOH}) = 0.0001$ g/g in the case of the calibration factor determination (sequence (B)).

3.3. Mass spectrometry

One experimental run was divided into sequence (A) for the measurement of the "Si28" samples and respective IDMS blends using a static cup configuration with C and H3 only, and sequence (B) for the determination of the calibration factors (using natural silicon, "Si29", and "Si30") with all three Faraday cups in use. Prior to each sequence, the instrument was tuned and mass scans were performed in order to obtain best parameters for isotope amount ratio measurements and to check for possible molecular interferences as is described in [8]. All relevant mass interferences were resolved at least by using the high resolution mode. A typical mass scan of the "Si28" material (^{29}Si range) in the high resolution mode ($M/\Delta M = 8000$) is shown in Fig. 2a. The $^{29}Si^+$ signal in the "28Si" material is represented by a first rather small plateau followed by the interferences $^{28}Si^1H^+$, $^{12}C^{16}O^1H^+$, and $^{14}N_2{}^1H^+$. In contrast, the scan of the blank solution (aqueous NaOH, $w(\mathrm{NaOH}) = 0.001$ g/g) in that mass region displays only the interferences $^{12}C^{16}O^1H^+$, and $^{14}N_2{}^1H^+$ in a significant amount. Fig. 2b displays a scan of the "Si28" material in the range of ^{30}Si under equal conditions as shown in Fig. 2a. The spectrum is dominated by the very intense $^{14}N^{16}O^+$ signal. However, an enlargement (as displayed in the inset) clearly shows the $^{30}Si^+$ signal before the onset of the large interference. The blank solution (aqueous NaOH, $w(\mathrm{NaOH}) = 0.001$ g/g) was scanned under the same conditions. The use of the Neptune MC-ICP-MS benefits from the ability to switch between three different fixed resolutions [23,24]. In the case of natural silicon used to determine the calibration factors, hydride formation ($^{28}Si^1H^+$ and $^{29}Si^1H^+$) could not be observed. For this reason, the experiments of sequence (B) using natural silicon were performed in the medium resolution mode in order to benefit from the higher transmission. In the case of the measurements of "Si28" (sequence (A)), however, extreme care must be taken in order to separate the $^{29}Si^+$ and $^{30}Si^+$ signal from their corresponding hydrides $^{28}Si^1H^+$ and $^{29}Si^1H^+$. This material generates significant hydride interferences due to the extreme enrichment in ^{28}Si. Therefore, the "Si28" isotope amount ratio measurements were performed in the high resolution mode which enables a proper separation of the silicon signal from the hydrides. A more detailed discussion is presented below. The plasma was in operation during the entire run of sequences (A) and (B). In between (A) and (B), the cup configuration was changed as described. In sequence (A) the solutions of the "Si28" material (x), and the IDMS blend (bx) ("Si28" plus "Si30") were subdivided into three aliquots. Each of them was transferred into a separate sample vial of the autosampler. The initial solutions (x) and (bx) were measured four times. Each sample measurement was bracketed by two blank measurements using exactly the same conditions. Fig. 3 schematically shows the arrangement of blank and sample measurement in sequence (A). The measurement procedure of sequence (B) using natural silicon for the determination of the calibration factors was described in [8]. It must be noted that in the case of a combined measurement of "Si28" and the calibration factor measurement as in the current work, the notation was changed in one detail: Here, the materials "Si30", "Si29", and natural silicon are indicated as y, z, and w, in contrast to [8]. Using the Neptune software (version 3.2.0.14), sequence (A) starts around 11 a.m. after running the Neptune for 2 h to reach stable working conditions. Sequence (B) then starts around 6 p.m. and takes approximately additional 6 h. When measuring two different samples (e.g. "Si28"-5 and "Si28"-8) in sequence (A) it consists of 16 sample measurements ("Si28"-5, "Si28"-8 and the respective IDMS blends bx-5 and bx-8) and at least 18 blank measurements. A sample (or blank) measurement consists of 60 s take-up time, the isotope amount ratio determination within the chosen method and 180 s wash time. The methods used for sequence (A) were the same as in sequence (B) [8], except for a different cup configuration: only cups C and H3 were used. All experiments were carried out using the *Virtual Amplifier concept* of the Neptune [23]. The parameters used and data evaluation performed in sequence (B) were described in [8]. With this arrangement it was possible to substract the measured blank isotope signal (containing contaminations of

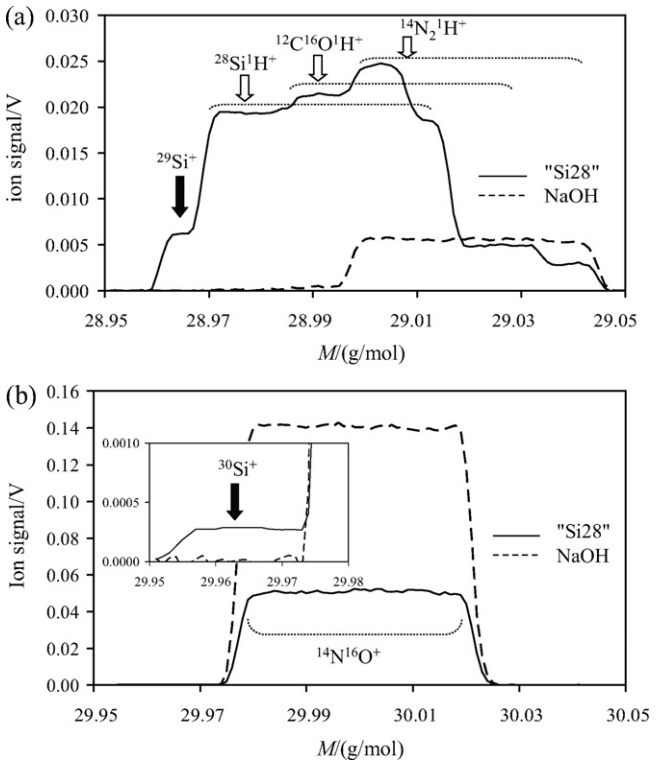

Fig. 2. (a) High resolution (HR) mass scan ($M/\Delta M = 8000$) of "Si28" ($w(\mathrm{Si}) = 4000$ μg/g; $w(\mathrm{NaOH}) = 0.001$ g/g) using the Neptune's central Faraday cup in the range of ^{29}Si. Note the small plateau of $^{29}Si^+$ followed by the interferences (dotted curly brackets) of $^{28}Si^1H^+$, $^{12}C^{16}O^1H^+$, and $^{14}N_2{}^1H^+$. The "Si28" spectrum is compared to the blank solution (aqueous NaOH, $w(\mathrm{NaOH}) = 0.001$ g/g). (b) HR mass scan under the same conditions as in (a) in the range of ^{30}Si. The spectrum is dominated by the large $^{14}N^{16}O^+$ interference signal. The enlarged inset shows the plateau of $^{30}Si^+$.

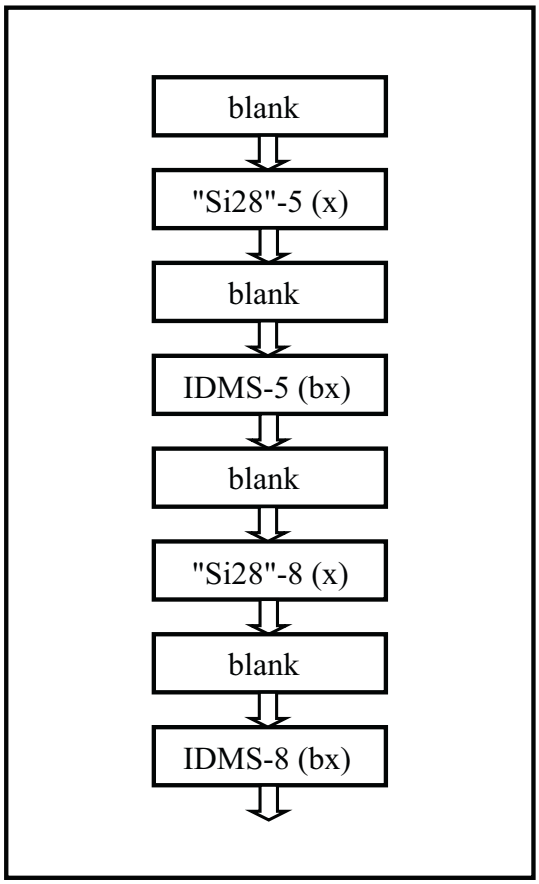

Fig. 3. Schematic course of the measurement of "Si28" (x) and the IDMS blend (bx) in sequence (A) using two different "Si28" crystal materials (e. g. "Si28"-5 and "Si28"-8). The silicon samples were bracketed by blank measurements (NaOH; $w(\mathrm{NaOH}) = 0.001$ g/g). In each sample and blank the ion voltages ($U(^{29}\mathrm{Si})$, $U(^{30}\mathrm{Si})$) were measured in exactly the same way. The sequence was performed twice in the forward direction and twice in the reverse direction. The total duration of sequence (A) is approximately 3–6 h depending on the number (one or two) of different "Si28" samples.

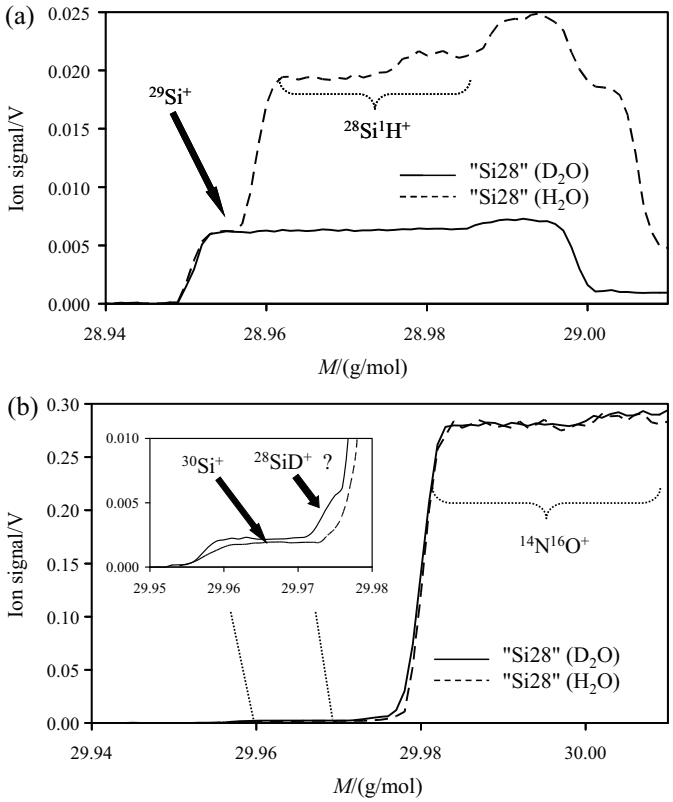

Fig. 4. (a) High resolution (HR) mass scan ($M/\Delta M = 8000$) of "Si28" using the Neptune's central Faraday cup in the range of ^{29}Si. A scan of an "Si28" sample dissolved in the system $NaOH/H_2O$ (dotted curve) is plotted vs. a scan of an "Si28" sample dissolved in the system $NaOH/D_2O$ (solid line). The spectra show first the small plateau of $^{29}Si^+$ followed by the interferences. In the case of "Si28" dissolved in $NaOH/H_2O$ a strong hydride signal $^{28}Si^1H^+$ appears and completely disappears in the case using the $NaOH/D_2O$ system. (b) HR mass scan under the same conditions as (a) in the range of ^{30}Si. The spectra show first the small plateaus of $^{30}Si^+$ followed by interferences. In the case of "Si28" dissolved in an $NaOH/D_2O$ system, a weak "tail" indicates the formation of a $^{28}SiD^+$ signal.

natural silicon, "Si29", or "Si30") from the respective sample signal which is one of the main advantages of the Neptune MC-ICP-MS. This blank correction comprised mainly the contamination by the used blank (aqueous NaOH) itself, the contamination influence of the vial material, and the memory of mainly the ICP-MS sample introduction.

3.4. Hydride interferences

When investigating the "Si28" material we observed the formation of an intense $^{28}Si^1H^+$ interference signal right after the occurance of the $^{29}Si^+$ signal (compare Fig. 2a). The hydrides can be resolved properly in the high resolution mode. The appearance of the most important $^{28}Si^1H^+$ hydride signal was investigated by an alternative preparation route. An "Si28" sample was dissolved in aqueous NaOH on the basis of D_2O instead of H_2O. For this purpose, D_2O (Merck, 99.9%, NMR grade) was used instead of H_2O. A proton/deuterium exchange then opresses the formation of the hydride signal. This fact is displayed in Fig. 4a. In the deuterated system only the $^{29}Si^+$ signal could be detected in the beginning of the spectrum and the $^{28}Si^1H^+$ signal was missing. In the H_2O solvated system on the other hand, a clear $^{28}Si^1H^+$ hydride signal appeared which was separated by a molar mass difference of 8.25×10^{-3} g/mol from the $^{29}Si^+$ signal. The $^{30}Si^+$ signal was followed by a strong and dominating $^{14}N^{16}O^+$ signal as reported in [25] and [26]. The problem of signal tailing effects is discussed later. Fig. 4b shows a comparison of mass scans of "Si28" samples in the ^{30}Si range dissolved in the $NaOH/H_2O$ and $NaOH/D_2O$ systems. In the range of ^{30}Si, a possible $^{29}Si^1H^+$ signal could not be detected. This would have a difference in molar mass of 0.0105 g/mol with respect to the lighter $^{30}Si^+$. When analyzing the deuterated system a $^{28}SiD^+$ (D = ^{2}H) signal might be expected. This has a difference in molar mass of 0.017 g/mol compared to the $^{30}Si^+$ signal. A small "tail" right on the onset of the $^{14}N^{16}O^+$ signal suggests the appearance of such a signal. However, it was of no significance for the measurements of the isotope amount ratios of this work. The analysis of the hydride interferences was completed by an investigation of the plateau width of the very small $^{29}Si^+$ plateau. This was done according to [24] by measuring the isotope amount ratios $R(^{30}\mathrm{Si}/^{29}\mathrm{Si})$ backwards and forwards from the center of the $^{29}Si^+$ plateau in steps of 0.0005 g/mol. A plateau width of 50 ppm ($\Delta M/M$) corresponding to a molar mass range of 0.0015 g/mol was obtained. Within this range $u_{\mathrm{rel}}(R(^{30}\mathrm{Si}/^{29}\mathrm{Si}))$ was smaller by 2%, sufficient for the determination of the molar mass with $u_{\mathrm{rel}}(M) \leq 1 \times 10^{-8}$. The instrumental drift in molar mass was $\leq$0.0005 g/mol/(24 h), allowing a proper measurement of $R(^{30}\mathrm{Si}/^{29}\mathrm{Si})$.

3.5. Proof of the $^{30}Si^+$ signal

One major problem during the investigation of the molar mass of the highly enriched "Si28" material is the

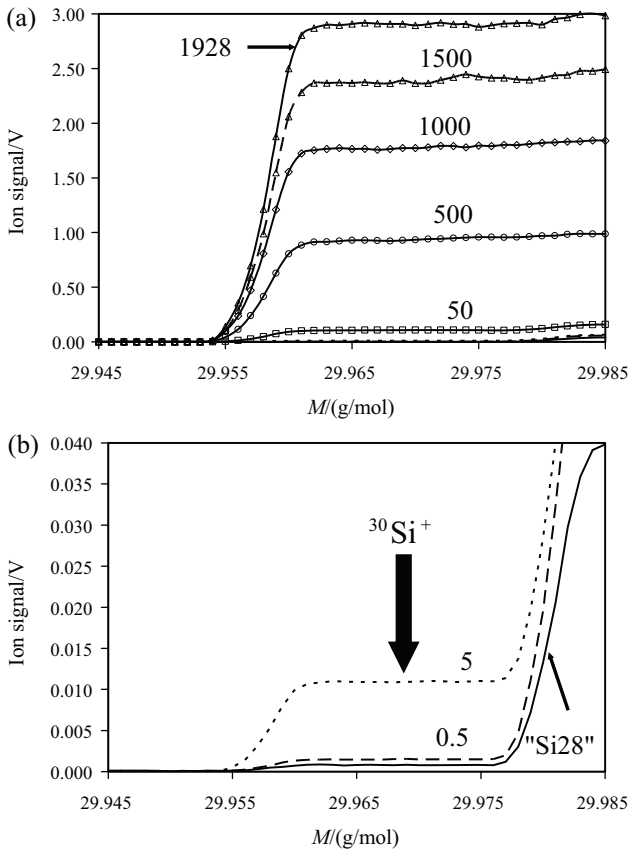

Fig. 5. High resolution mass scans ($M/\Delta M = 8000$) of blends containing "Si28", "Si29", and "Si30" using the Neptune H3 Faraday cup in the range of ^{30}Si. The numbers indicate the respective total silicon mass fractions of the blends. As can be seen, the signal intensity of the $^{30}Si^+$ plateau decreased proportional to the respective mass fraction of silicon. In (a) the higher concentrated blends are shown. Due to the high mass fractions of silicon, the $^{14}N^{16}O^+$ interference merges with the $^{30}Si^+$ signal and cannot be detected clearly. In (b) this onset of the subsequent $^{14}N^{16}O^+$ interference is clearly apparent. The lowest curve corresponds to the pure "Si28" sample.

extremely low amount-of-substance fraction of the ^{30}Si isotope ($x(^{30}Si) \approx 1.3 \times 10^{-6}$ mol/mol). This generates a signal of considerably weak intensity (usually <1 mV). This problem is connected with the subsequent appearance of the large $^{14}N^{16}O^+$ interference which is a consequence of entrained atmospheric gases. Engström et al. [25] have observed a considerable tailing effect due to this interference which might influence the $^{30}Si^+$ signal. The influence of signal tailing in our work is discussed below. Therefore, we must ensure that we "really" measure the $^{30}Si^+$ signal and not an artefact. For these investigations we have prepared blends of several graded concentrations of ^{30}Si. The blends were made by mixing initially "Si28" ($w = 3800\ \mu g/g$, $w(NaOH) = 0.001$ g/g), "Si29" ($w = 46\ \mu g/g$, $w(NaOH) = 0.001$ g/g), and "Si30" ($w = 155\ \mu g/g$, $w(NaOH) = 0.001$ g/g). Then, a blend (stock solution) with a total silicon concentration of $w = 1928\ \mu g/g$ ($w(NaOH) = 0.001$ g/g) was prepared. This generated an expected isotope amount ratio $R(^{30}Si/^{29}Si)$ of ≈3.7. This stock solution was diluted gradually to form silicon blends with total silicon mass fractions $w = 1500$, 1000, 500, 50, 5, and 0.5 μg/g ($w(NaOH) = 0.001$ g/g). The measured $^{30}Si^+$ signals gradually decreased proportional to those mass fractions. Fig. 5a and b displays this gradual decrease of the very $^{30}Si^+$ signal which was compared to the respective $^{30}Si^+$ signal of the "Si28" sample (lowest curve in Fig. 5b). This was a clear indication and proof of the origin of the $^{30}Si^+$ signal.

Table 1
Total silicon concentrations in different NaOH matrices formed by the blend described in Section 3.7. The measured $R(^{30}Si/^{29}Si)$ are indicated with respective associated uncertainties.

Dilution	w(Si)/(μg/g)	w(NaOH)/(g/g)	$R(^{30}Si/^{29}Si)$/(V/V)	$u(R)$/(V/V)
Stock	1928	0.00120	3.6992	0.0025
1	1500	0.00093	3.7016	0.0003
2	1000	0.00048	3.7057	0.0004
3	50	0.00120	3.7106	0.0055
4	5	0.00012	3.7047	0.0199

3.6. Investigation of tailing effects on the $^{29}Si^+$ and $^{30}Si^+$ signals

A tailing of a very intense signal can influence the signal plateau under investigation by superposition. In the current work, care must be taken in this regard when studying ^{29}Si and ^{30}Si by isotope amount ratio measurements. The $^{29}Si^+$ signal could be influenced by the very intense, but not detected $^{28}Si^+$ signal, while the $^{30}Si^+$ signal might be influenced by the strong $^{14}N^{16}O^+$ interference as reported by Engström et al. [25] and van den Boorn et al. [26]. In order to investigate these probabilities, the ion currents were measured at two positions, lb1 and lb2 (lb denotes the "background" signal at the lower mass side), on the low mass side of the $^{29}Si^+$ and the $^{30}Si^+$ signal itself. The mass settings in those runs were: lb1(^{29}Si) = 28.950 g/mol, lb2(^{29}Si) = 28.958 g/mol, C(^{29}Si) = 28.968 g/mol. This was possible by using a special feature of the Neptune MC-ICP-MS in the cup configuration setting (usually cups C and H3 were used): an additional "sub" cup configuration (here, lb1 and lb2 can be programmed with respect to C and H3, each). The same procedure was done for the $^{30}Si^+$ signal (mass settings: lb1(^{30}Si) = 29.925 g/mol, lb2(^{30}Si) = 29.935 g/mol, H3(^{30}Si) = 29.950 g/mol). All these six masses were measured "quasi" simultaneously in the static high resolution mode. After this, linear regressions were performed using the pairs lb1(^{29}Si), lb2(^{29}Si) and lb1(^{30}Si), lb2(^{30}Si). For each region these regression curves were extrapolated into the C and H3 mass, respectively. The respective ordinate (signal intensity) at C and H3 should indicate the amount of the tailing signal which must be corrected for by subtracting it from the original signal at this very point. For both ranges – $^{29}Si^+$ and $^{30}Si^+$ – we did not observe this kind of additional tailing signal. Therefore, we can conclude that tailing in the case of both signals could be neglected in our measurements.

3.7. Dependence of K factors and isotope amount ratios on total silicon and matrix concentration

As described in Section 3.3, a total measurement of one sample was divided into two sequences: (A) for the measurement of the "Si28" sample and (B) for the measurement of the calibration factors. As explained, in (A) the total silicon concentration of the "Si28" samples was $w \approx 4000\ \mu g/g$ ($w(NaOH) = 0.001$ g/g), and in (B) each sample of natural silicon (w), "Si29" (z), "Si30" (y), and the blends b1 and b2 had silicon concentrations of $w = 4\ \mu g/g$ ($w(NaOH) = 0.0001$ g/g). We have performed experiments in order to guarantee that these large differences in silicon and matrix concentrations did not influence the isotope amount ratios $R(^{30}Si/^{29}Si)$ and the calibration factors K_{30} and K_{28}. For this purpose, the stock solution described in Section 3.5 with $w(Si) = 1928\ \mu g/g$ ($w(NaOH) = 0.001$ g/g) was diluted with H_2O in order to prepare solutions with decreasing and graded silicon and NaOH concentrations. Table 1 summarizes the mass fractions w of total silicon in the respective solutions together with the respective NaOH concentrations. These solutions cover the range of several orders of magnitude in concentration of the solutions used in the molar mass determinations of the "Si28" material as shown in Fig. 6a. No significant influence from both the silicon concentrations and the NaOH

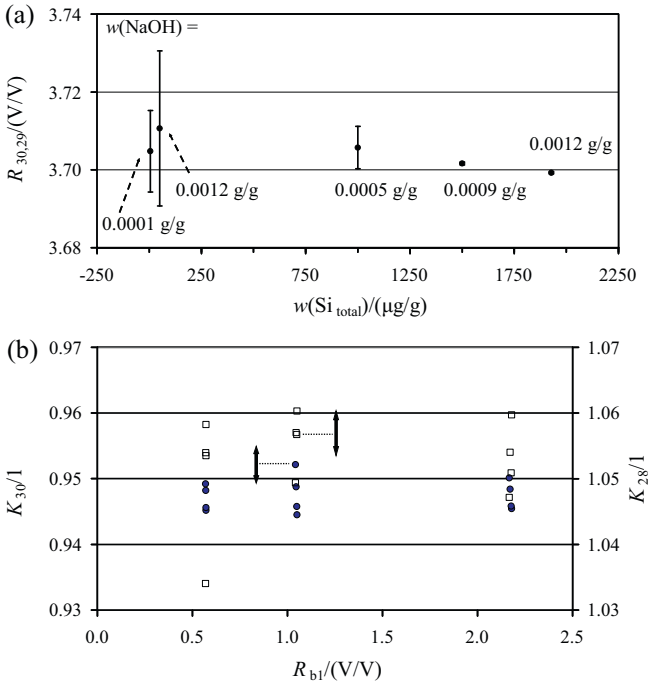

Fig. 6. (a) Isotope amount ratios $R(^{30}Si/^{29}Si)$ with associated standard uncertainties of blends made of "Si28", "Si29", and "Si30" as a function of the total silicon concentration and NaOH concentration. Note that the first (w(Si) = 5 µg/g, w(NaOH) = 0.0001 g/g) and last (w(Si) = 1928 µg/g, w(NaOH) = 0.0012 g/g) data points correspond approximately to the real used concentrations in sequences (A) and (B). (b) Calibration factors K_{30} (left scale, filled circles) and K_{28} (right scale, open squares) were determined with blend b1 of three different isotope amount ratios $R(^{30}Si/^{29}Si)$. The arrows indicate the mean expanded measurement uncertainties for K_{30} and K_{28}.

concentrations can be observed with respect to $R(^{30}Si/^{29}Si)$ and their associated uncertainties (and indirectly the K factors). This legitimates the use of concentrations which differ in sequences (A) and (B).

3.8. Dependence of K factors on isotope amount ratios of blends b1 and b2

The calibration factor determination was described in detail in [7,9]. In the case of the "Si28" measurements, Fig. 1a schematically shows the way how the blends necessary for the experimental K factor determination were prepared. The isotope amount ratios R_{b1} and R_{b2} were chosen as equal as unity as possible. This was accomplished by mixing solutions of "Si30" and "Si29" for the b1 blend and mixing solutions of "Si29" and natural silicon in the case of the b2 blend, respectively. We have investigated a possible influence of the deviation of the respective isotope amount ratios on the calibration factors and their associated uncertainty. Blends were prepared for b1 exemplarily, resulting in $R(^{30}Si/^{29}Si) \approx 0.5$, 1, and 2 V/V. Fig. 6b shows the distribution of K_{30} (left scale) and K_{28} (right scale) with associated expanded uncertainties for three different $R(^{30}Si/^{29}Si)$. No significant influence of variations of that isotope amount ratio on K_{30}, K_{28}, and their associated uncertainties has been observed.

3.9. Dependence of K factors on resolution

To be allowed to correct the isotope amount ratios measured in sequence (A) applying the K factors determined in (B), it is crucial to ensure that the K factors are independent of the resolution chosen, since in sequences (A) and (B) different resolutions were used (HR and MR, respectively). This was experimentally proven by measuring the isotope amount ratios $R(^{30}Si/^{29}Si)$ and $R(^{28}Si/^{29}Si)$ in the MR and HR mode using a natural silicon sample (w(Si) = 4 µg/g). Eight measurements in total were performed alternately (MR, HR, MR, HR, etc.). Fig. 7 shows normalized isotope amount ratios with associated standard uncertainties. Due to higher ion signal intensities, the standard uncertainties measured in the MR mode are smaller compared to those measured in the HR mode. The ranges of the standard deviations of the MR and HR measurements overlap. This simple experiment shows that switching between the MR and HR mode, only, does not significantly influence the K factors.

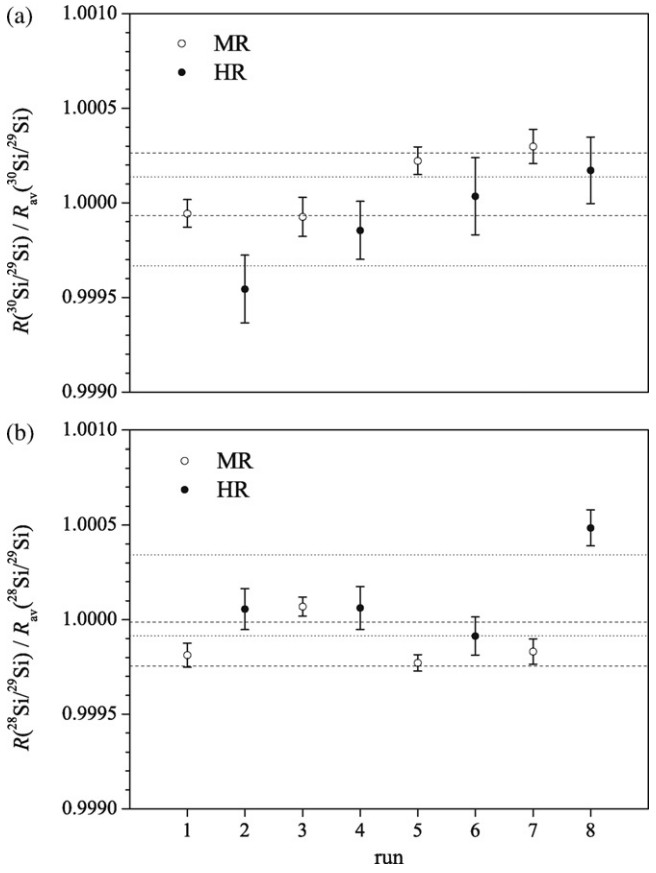

Fig. 7. (a) Normalized isotope amount ratios $R(^{30}Si/^{29}Si)$ with associated standard uncertainties of natural silicon measured in the medium resolution mode (MR) and high resolution mode (HR) during eight runs. All other parameters were kept constant. The standard deviations of MR are given by dashed lines, those of HR are indicated by dotted lines. Normalization was done by dividing the repective isotope amount ratio with the average isotope amount ratio. (b) Same as (a) for $R(^{28}Si/^{29}Si)$.

4. Results and discussion

Molar mass measurements have been performed using crystal samples of parts 4, 5, 8, and 9 of the "Si28" ingot. Fig. 8 shows the distribution of the molar mass obtained by measurements of seven different samples along the crystal axis (the notation indicates the origin of each sample). The single values (filled circles) are the arithmetic means of the respective sample measurements. Error bars display the respective associated combined measurement uncertainties with a coverage factor of $k = 1$. The bold dashed line corresponds to the arithmetic mean molar mass of the seven samples. The respective numerical values and amount-of-substance fractions $x(^{i}Si)$ are listed in Table 2. Additionally, the mean values of the samples from parts 5 and 8 are listed. The final molar mass and isotopic abundance of the "Si28" crystal is given in the last row of Table 2 as an average of the measurements from parts 5 and 8. The mean molar mass of the "Si28" silicon crystal material is M(Si) = 27.97697027(23) g/mol with an associated relative uncer-

Table 2
Molar mass M and isotopic abundances (amount-of-substance fractions) $x(^{i}\mathrm{Si})$ of "Si28" silicon crystal samples (arithmetic mean of each sample)

Molar mass and isotopic composition: "Si28" silicon crystal					
i	Sample	M/(g/mol)	$x(^{28}\mathrm{Si})$/(mol/mol)	$x(^{29}\mathrm{Si})/(10^{-5}$ mol/mol)	$x(^{30}\mathrm{Si})/(10^{-6}$ mol/mol)
1	4.4	27.97697030(28)	0.99995748(24)	4.122(23)	1.30(3)
2	5.B2.1.4	27.97697009(20)	0.99995764(14)	4.111(12)	1.25(4)
3	5.B3.1.1.3	27.97697039(23)	0.99995738(16)	4.132(14)	1.30(5)
4	5.B4.1.1.4	27.97697035(23)	0.99995741(18)	4.132(16)	1.27(4)
5	8.A2.1.4	27.97697006(24)	0.99995768(17)	4.104(14)	1.28(5)
6	8.B4.1.1.3	27.97697047(24)	0.99995733(19)	4.135(17)	1.32(4)
7	9.8	27.97697033(21)	0.99995740(16)	4.134(14)	1.26(4)
8	$\frac{1}{3}\sum_{i=2}^{4} M_i$	27.97697028(22)	0.99995750(16)	4.123(14)	1.27(4)
9	$\frac{1}{2}\sum_{i=5}^{6} M_i$	27.97697027(24)	0.99995751(18)	4.119(16)	1.30(4)
	$\frac{1}{2}\sum_{i=8}^{9} M_i$	27.97697027(23)	0.99995750(17)	4.121(15)	1.29(4)

Their respective combined measurement uncertainties u are given in brackets (last digits).

tainty $u_{\mathrm{rel}} = 8.2 \times 10^{-9}$ for $k = 1$. The relative standard deviation with respect to the mean of all measurements is $s_{\mathrm{rel}} = 3.5 \times 10^{-9}$. All averaged sample data displayed in Fig. 7 are located inside the band defining the combined measurement uncertainty with k = 1. Compared with the overall standard deviation s_{rel} this result reflects a degree of homogeneity with respect to the molar mass that underpins the suitability of the "Si28" material to be used for the determination of N_{A}. Even the two outermost samples from parts 4 and 9 are covered by the k = 1 interval. The measurement uncertainty obtained now even comes below the intended limit of the measurement uncertainty $u_{\mathrm{rel}} = 1 \times 10^{-8}$ of the molar mass. This exceeds the requirement of the Avogadro project for the reassessment of N_{A} with the intention of $u_{\mathrm{rel}}(N_{\mathrm{A}}) \leq 1 \times 10^{-8}$ and also the prediction of the feasibility study of part 1, claiming a possible uncertainty of the molar mass of $u_{\mathrm{rel}} = 1.7 \times 10^{-8}$ [7].

Fig. 9 gives an overview of all 29 single experiments performed so far with the samples listed above. No systematic tendency concerning the homogeneity of the crystal can be observed. Each data point (filled circle) was obtained as a combination of the sequences (A) and (B) measured during one day. The general course of data distribution suggests a formal statistical behaviour. Table 3 displays a representative uncertainty budget of a crystal sample of the "Si28" material according to the Guide to the Expression of Uncertainty in Measurement [27]. Three main uncertainty contributions can be identified: the largest with a contribution of 46% is related to the isotope amount ratio R_{x} which is the ratio $R(^{30}\mathrm{Si}/^{29}\mathrm{Si})$ of the "Si28" sample itself. This demonstrates that it is sufficient to measure this isotope amount ratio with a relative uncertainty better than approximately 5%. Another large uncertainty contribution with 20% is produced by the isotope amount ratio R_{bx}, which is the corresponding ratio $^{30}\mathrm{Si}/^{29}\mathrm{Si}$ in the blend bx prepared from the "Si28" sample and the spike material ("Si30"). The contribution of the calibration factor K_{30} with 7.7% is of minor importance at this stage. The limit of uncertainty achievable with the applied method is becoming obvious when regarding the second largest uncertainty contribution of 23%: the molar mass $M(^{28}\mathrm{Si})$. This value was taken from [17]. However, as discussed in Section 2, a new value with reduced uncertainty is available, but it is not used here for the sake of a more conservative uncertainty budget. Compared to the uncertainty budget of the molar mass of natural silicon [8], the influence of the uncertainties of the masses and mass fractions is negligible. The main and predicted result is the reduction of measurement uncertainty of the molar mass by at least two orders of magnitude when investigating the "Si28" material instead of natural silicon (both by means of MC-ICP-MS [8]). What is the intrinsic reason for this special material-dependent behaviour? The answer is mainly

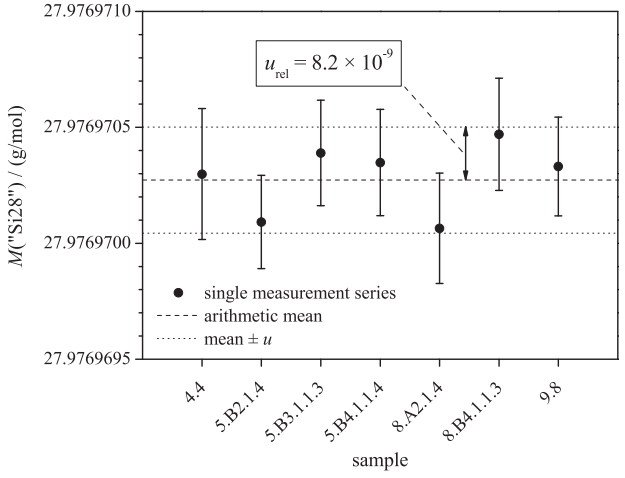

Fig. 8. Molar mass distribution of "Si28" samples (7 samples of different origin within the float zone ingot). The displayed relative combined uncertainty $u_{\mathrm{rel}} = 8.2 \times 10^{-9}$ (k = 1) was derived from parts 4, 5, 8, and 9. Each data point (filled circle) is the average of a series of respective molar mass measurements of approximately two weeks. Error bars indicate the respective combined measurement uncertainty (k = 1). Bold dashed line: arithmetic mean value; dotted lines: combined uncertainty of the mean value.

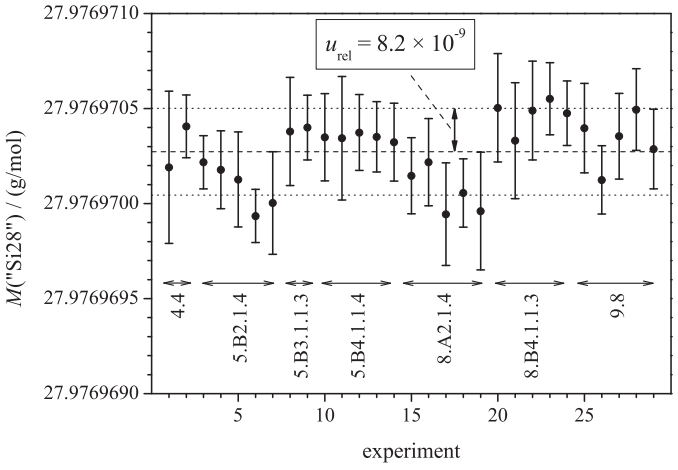

Fig. 9. Molar mass distribution of the single measurements of the "Si28" samples (the exact origin from the float zone crystal is indicated). The displayed relative combined uncertainty $u_{\mathrm{rel}} = 8.2 \times 10^{-9}$ (k = 1) was derived from parts 4, 5, 8, and 9. Each data point (filled circle) is obtained by a single measurement (one day) as a combination of sequences (A) and (B). Error bars indicate the respective combined measurement uncertainty (k = 1). Bold dashed line: arithmetic mean value; dotted lines: combined uncertainty of the mean value.

Table 3
Uncertainty budget of the molar mass M of the "Si28" crystal material used for the reassessment of the Avogadro constant (N_A).

Quantity X_i	Unit $[X_i]$	Best estimate (value) x_i	Standard uncertainty $u(x_i)$	Sensitivity coefficient c_i	Index
$x_x(^{28}Si)$	mol/mol	0.99995753	1.6×10^{-7}		
$x_x(^{29}Si)$	mol/mol	4.119×10^{-5}	1.3×10^{-7}		
$x_x(^{30}Si)$	mol/mol	1.28×10^{-6}	6×10^{-8}		
$M(^{28}Si)$	g/mol	27.97692649	1.10×10^{-7}	1.0	23.1
$M(^{29}Si)$	g/mol	28.97649468	1.10×10^{-7}	4.1×10^{-5}	0.0
$M(^{30}Si)$	g/mol	29.97377018	1.10×10^{-7}	0.0	0.0
w_{imp}	g/g	4.40×10^{-5}	1.6×10^{-7}		
w_y	g/g	9.978×10^{-7}	7×10^{-10}		
R_x	mol/mol	0.03273	1.4×10^{-3}	1.1×10^{-4}	46.3
R_y	mol/mol	219.34	4.62	3.1×10^{-9}	0.4
R_{bx}	mol/mol	1.36630	3.12×10^{-3}	-3.3×10^{-5}	20.3
K_{30}	1	0.94991	1.48×10^{-3}	-4.30×10^{-5}	7.7
$R_{y,28}$	mol/mol	1.021	0.115	-200×10^{-9}	1.0
K_{28}	1	1.04378	9.82×10^{-3}	-200×10^{-9}	0.0
m_{yx}	g	7.26650×10^{-6}	0.00409×10^{-6}	5.7	1.2
m_x	g	0.12798	1.2×10^{-5}	-3.4×10^{-4}	0.0

Y	$[Y]$	y	$u_c(y)$	$u_{rel}(y)$
M(Si)	g/mol	27.97697022	2.29×10^{-7}	8.2×10^{-9}

Displayed is a representative budget from a sample originating from part 8 of the crystal. The budget has been calculated using the *GUM-Workbench* software [28]. The listed quantities are explained in part 1 [7] and the notation was used according to [29]. The quantity m_{yx} in this table denotes the mass of the spike (y) used for the preparation of the IDMS blend bx. Standard uncertainties are given for $k = 1$. The unit of the sensitivity coefficients c_i is $[c_i] = \text{g/mol}/[X_i]$ (not displayed for more clarity). The column "Index" shows the relative uncertainty contribution (in %) of the respective input quantity X_i to the molar mass M(Si) of the highly enriched "Si28" material which is the final output quantity Y. The blank cells for c_i and Index result from intermediate results which were no real input quantities for the budget. The isotope amount ratios R were already corrected with respect to the background and contamination through subtracting the blank values as described above. The combined measurement uncertainty u_c is given for $k = 1$.

connected with the isotopic abundance of ^{29}Si and ^{30}Si in "Si28". The amount-of-substance fraction $x_x(^{29}Si)$ is aproximately 32 times larger than $x_x(^{30}Si)$. This enables an effective spiking with a material highly enriched in ^{30}Si as "Si30". The application of the modified IDMS method to the "Si28" material using the virtual element will reduce the overall uncertainty in M drastically. In contrast, using natural silicon $x_x(^{29}Si)$ is only 1.5 times larger than $x_x(^{30}Si)$. Applying IDMS with that arrangement cannot yield a relative uncertainty in the 10^{-8} range.

5. Conclusions

This work intended to determine the molar mass of the silicon crystal material highly enriched in ^{28}Si ("Si28"), completes a series of investigations, starting with the theoretical derivations and a feasibility study [7], and applying the new experimental methods successfully using natural silicon [8]. In the current study, the molar mass of "Si28" has been measured for the first time applying the combination of a modified IDMS method and an MC-ICP-MS. One prominent experimental advantage was the ability to correct the isotope amount fractions measured using the blank data including all contributions of contamination. Moreover, the new preparation technique has proven itself, because of minimizing the strong influence of contamination with silicon other than the "Si28" material. The final measurement uncertainty associated with the molar mass of silicon has been reduced by more than one order of magnitude when investigating the "Si28" material (using MC-ICP-MS) instead of natural silicon (using gas mass spectrometry [30]). This was a major prerequisite in the advancement of the Avogadro project as has been predicted in [31]. Ending up in the reported measurement uncertainty of the molar mass of "Si28" it is possible to reassess N_A with a relative measurement uncertainty $u_{rel}(N_A) \leq 3 \times 10^{-8}$ at the moment [32]. Further experiments intending to screen the nature of the "Si28" crystal with respect to the molar mass are under way. A combination with other sophisticated methods such as Laser-Ablation-ICP-MS (LA-ICP-MS) or time-of-flight (TOF) methods for systems with larger molar mass will be a challenge in the near future, too.

Acknowledgements

The authors gratefully acknowledge fruitful discussions with Giovanni Mana (INRIM), Rüdiger Kessel (NIST), and Horst Bettin (PTB). Sincere thanks to Michael Deerberg and Johannes B. Schwieters (both Thermo Fisher Scientific) for discussions and the release of material on the resolution capabilities of the Neptune mass spectrometer. We thank Ursula Schulz (PTB) for her sedulous assistance during the preparation of the chemical solutions. The research within this EURAMET joint research project receives funding from the European Community's Seventh Framework Programme, ERA-NET Plus, under Grant Agreement No. 217257.

Appendix A.

Starting from Eqs. (4)–(8), taken from [7], a more compact and simplified equation for the direct calculation of the molar mass M was derived with the intention to render intermediate results obsolete and this way reducing possible machine errors.

$$x_x(^{28}Si) = \frac{(1 - w_{imp})/M(^{28}Si)}{(1 - w_{imp})/M(^{28}Si) + (1 + R_x)w_{imp}/(M(^{29}Si) + R_x M(^{30}Si))} \quad (4)$$

$$x_x(^{29}Si) = \frac{w_{imp}/(M(^{29}Si) + R_x M(^{30}Si))}{(1 - w_{imp})/M(^{28}Si) + (1 + R_x)w_{imp}/(M(^{29}Si) + R_x M(^{30}Si))} \quad (5)$$

$$x_x(^{30}Si) = \frac{R_x w_{imp}/(M(^{29}Si) + R_x M(^{30}Si))}{(1 - w_{imp})/M(^{28}Si) + (1 + R_x)w_{imp}/(M(^{29}Si) + R_x M(^{30}Si))} \quad (6)$$

$$w_{imp} = w_y \frac{m_{yx}}{m_x} \frac{M(^{29}Si) + R_x M(^{30}Si)}{M(^{29}Si) + R_y M(^{30}Si)} \frac{R_y - R_{bx}}{R_{bx} - R_x} \quad (7)$$

$$w_y = \frac{M(^{29}Si) + R_y M(^{30}Si)}{R_{y,28} M(^{28}Si) + M(^{29}Si) + R_y M(^{30}Si)} \quad (8)$$

Eqs. (4)–(6) in (9) yields:

$$M = x_x(^{28}Si)M(^{28}Si) + x_x(^{29}Si)M(^{29}Si) + x_x(^{30}Si)M(^{30}Si) \quad (9)$$

$$M = \frac{(M(^{28}\mathrm{Si})(1-w_{\mathrm{imp}}))/(M(^{28}\mathrm{Si})) + (M(^{29}\mathrm{Si})w_{\mathrm{imp}})/(M(^{29}\mathrm{Si}) + R_{\mathrm{x}}M(^{30}\mathrm{Si})) + (M(^{30}\mathrm{Si})R_{\mathrm{x}}w_{\mathrm{imp}})/(M(^{29}\mathrm{Si}) + R_{\mathrm{x}}M(^{30}\mathrm{Si}))}{(1-w_{\mathrm{imp}})/(M(^{28}\mathrm{Si})) + ((1+R_{\mathrm{x}})w_{\mathrm{imp}})/(M(^{29}\mathrm{Si}) + R_{\mathrm{x}}M(^{30}\mathrm{Si}))} \quad (10)$$

$$M = \frac{((M(^{28}\mathrm{Si})(1-w_{\mathrm{imp}})(M(^{29}\mathrm{Si}) + R_{\mathrm{x}}M(^{30}\mathrm{Si})) + M(^{28}\mathrm{Si})M(^{29}\mathrm{Si})w_{\mathrm{imp}} + M(^{28}\mathrm{Si})M(^{30}\mathrm{Si})R_{\mathrm{x}}w_{\mathrm{imp}})/(M(^{28}\mathrm{Si})(M(^{29}\mathrm{Si}) + R_{\mathrm{x}}M(^{30}\mathrm{Si}))))}{((1-w_{\mathrm{imp}})(M(^{29}\mathrm{Si}) + R_{\mathrm{x}}M(^{30}\mathrm{Si})) + (1+R_{\mathrm{x}})w_{\mathrm{imp}}M(^{28}\mathrm{Si}))/(M(^{28}\mathrm{Si})(M(^{29}\mathrm{Si}) + R_{\mathrm{x}}M(^{30}\mathrm{Si})))} \quad (11)$$

$$M = \frac{\left[M(^{28}\mathrm{Si})(M(^{29}\mathrm{Si}) + R_{\mathrm{x}}M(^{30}\mathrm{Si})) - w_{\mathrm{imp}}M(^{28}\mathrm{Si})(M(^{29}\mathrm{Si}) + R_{\mathrm{x}}M(^{30}\mathrm{Si})) + M(^{28}\mathrm{Si})M(^{29}\mathrm{Si})w_{\mathrm{imp}} + M(^{28}\mathrm{Si})M(^{30}\mathrm{Si})R_{\mathrm{x}}w_{\mathrm{imp}}\right]}{(1-w_{\mathrm{imp}})(M(^{29}\mathrm{Si}) + R_{\mathrm{x}}M(^{30}\mathrm{Si})) + (1+R_{\mathrm{x}})w_{\mathrm{imp}}M(^{28}\mathrm{Si})} \quad (12)$$

$$M = \frac{M(^{28}\mathrm{Si})(M(^{29}\mathrm{Si}) + R_{\mathrm{x}}M(^{30}\mathrm{Si}))}{(1-w_{\mathrm{imp}})(M(^{29}\mathrm{Si}) + R_{\mathrm{x}}M(^{30}\mathrm{Si})) + w_{\mathrm{imp}}M(^{28}\mathrm{Si})(1+R_{\mathrm{x}})} \quad (13)$$

$$M = \frac{M(^{28}\mathrm{Si})(M(^{29}\mathrm{Si}) + R_{\mathrm{x}}M(^{30}\mathrm{Si}))}{w_{\mathrm{imp}}(M(^{28}\mathrm{Si})(1+R_{\mathrm{x}}) - M(^{29}\mathrm{Si}) - R_{\mathrm{x}}M(^{30}\mathrm{Si})) + (M(^{29}\mathrm{Si}) + R_{\mathrm{x}}M(^{30}\mathrm{Si}))} \quad (14)$$

Eq. (8) in (7) results in:

$$w_{\mathrm{imp}} = \frac{M(^{29}\mathrm{Si}) + R_{\mathrm{y}}M(^{30}\mathrm{Si})}{R_{\mathrm{y},28}M(^{28}\mathrm{Si}) + M(^{29}\mathrm{Si}) + R_{\mathrm{y}}M(^{30}\mathrm{Si})} \times \frac{m_{\mathrm{yx}}}{m_{\mathrm{x}}} \frac{M(^{29}\mathrm{Si}) + R_{\mathrm{x}}M(^{30}\mathrm{Si})}{M(^{29}\mathrm{Si}) + R_{\mathrm{y}}M(^{30}\mathrm{Si})} \frac{R_{\mathrm{y}} - R_{\mathrm{bx}}}{R_{\mathrm{bx}} - R_{\mathrm{x}}} \quad (15)$$

$$w_{\mathrm{imp}} = \frac{m_{\mathrm{yx}}}{m_{\mathrm{x}}} \frac{M(^{29}\mathrm{Si}) + R_{\mathrm{x}}M(^{30}\mathrm{Si})}{R_{\mathrm{y},28}M(^{28}\mathrm{Si}) + M(^{29}\mathrm{Si}) + R_{\mathrm{y}}M(^{30}\mathrm{Si})} \frac{R_{\mathrm{y}} - R_{\mathrm{bx}}}{R_{\mathrm{bx}} - R_{\mathrm{x}}} \quad (16)$$

Introducing (16) in (14) yields the final equation to describe the molar mass M merely as function of measured or known values without the need to calculate intermediate results.

$$M = \frac{M(^{28}\mathrm{Si})(M(^{29}\mathrm{Si}) + R_{\mathrm{x}}M(^{30}\mathrm{Si}))}{[\,(M(^{28}\mathrm{Si})(1+R_{\mathrm{x}}) - M(^{29}\mathrm{Si}) - R_{\mathrm{x}}M(^{30}\mathrm{Si}))((M(^{29}\mathrm{Si}) + R_{\mathrm{x}}M(^{30}\mathrm{Si}))/(R_{\mathrm{y},28}M(^{28}\mathrm{Si}) + M(^{29}\mathrm{Si}) + R_{\mathrm{y}}M(^{30}\mathrm{Si}))) \times (m_{\mathrm{yx}}/m_{\mathrm{x}})((R_{\mathrm{y}} - R_{\mathrm{bx}})/(R_{\mathrm{bx}} - R_{\mathrm{x}})) + (M(^{29}\mathrm{Si}) + R_{\mathrm{x}}M(^{30}\mathrm{Si}))\,]} \quad (17)$$

$$M = \frac{M(^{28}\mathrm{Si})}{1 + (m_{\mathrm{yx}}/m_{\mathrm{x}})((M(^{28}\mathrm{Si})(1+R_{\mathrm{x}}) - M(^{29}\mathrm{Si}) - R_{\mathrm{x}}M(^{30}\mathrm{Si}))/(R_{\mathrm{y},28}M(^{28}\mathrm{Si}) + M(^{29}\mathrm{Si}) + R_{\mathrm{y}}M(^{30}\mathrm{Si})))((R_{\mathrm{y}} - R_{\mathrm{bx}})/(R_{\mathrm{bx}} - R_{\mathrm{x}}))} \quad (18)$$

References

[1] R. Gonfiantini, P. De Bièvre, S. Valkiers, P.D.P. Taylor, Measuring the molar mass of silicon for a better Avogadro constant: reduced uncertainty, IEEE Trans. Instrum. Meas. 40 (1997) 566–571.

[2] P. Becker, H. Bettin, H.-U. Danzebrink, M. Gläser, U. Kuetgens, A. Nicolaus, D. Schiel, P. De Bièvre, S. Valkiers, P. Taylor, Determination of the Avogadro constant via the silicon route, Metrologia 40 (2003) 271–287.

[3] P. Becker, Tracing the definition of the kilogram to the Avogadro constant using a silicon single crystal, Metrologia 40 (2003) 366–375.

[4] P. Becker, D. Schiel, H.-J. Pohl, A.K. Kaliteevski, O.N. Godisov, M.F. Churbanov, G.G. Devyatykh, A.V. Gusev, A.D. Bulanov, S.A. Adamchik, V.A. Gaava, I.D. Kovalev, N.V. Abrosimov, B. Hallmann-Seiffert, H. Riemann, S. Valkiers, P. Taylor, P. De Bièvre, E.M. Dianov, Large-scale production of highly enriched ^{28}Si for the precise determination of the Avogadro constant, Meas. Sci. Technol. 17 (2006) 1854–1860.

[5] P. De Bièvre, G. Lenaers, T.J. Murphy, H.S. Peiser, S. Valkiers, The chemical preparation and characterization of specimens for "absolute" measurements of the molar mass of an element, exemplified by silicon, for redeterminations of the Avogadro constant, Metrologia 32 (1995) 103–110.

[6] P. Becker, P. De Bièvre, K. Fujii, M. Glaeser, B. Inglis, H. Luebbig, G. Mana, Considerations on future redefinitions of the kilogram, the mole and of other units, Metrologia 44 (2007) 1–14.

[7] O. Rienitz, A. Pramann, D. Schiel, Novel concept for the mass spectrometric determination of absolute isotopic abundances with improved measurement uncertainty: Part 1—Theoretical derivation and feasibility study, Int. J. Mass Spectrom. 289 (2010) 47–53.

[8] A. Pramann, O. Rienitz, D. Schiel, B. Güttler, Novel concept for the mass spectrometric determination of absolute isotopic abundances with improved measurement uncertainty: Part 2—Development of an experimental procedure for the determination of the molar mass of silicon using MC-ICP-MS, Int. J. Mass Spectrom. 299 (2011) 78–86.

[9] G. Mana, O. Rienitz, The calibration of Si isotope-ratio measurements, Int. J. Mass Spectrom. 291 (2010) 55–60.

[10] P. De Bièvre, Isotope dilution mass spectrometry: What can it contribute to accuracy in trace analysis? Fresenius J. Anal. Chem. 337 (1990) 766–771.

[11] K.G. Heumann, Isotope Dilution Mass Spectrometry, in: F. Adams, R. Gijbels, R. van Grieken (Eds.), Inorganic Mass Spectrometry, John Wiley & Sons, New York, 1988, pp. 301–376.

[12] K.G. Heumann, Isotope dilution mass spectrometry, Int. J. Mass Spectrom. Ion Processes T 118/119 (1992) 575–592.

[13] K.G. Heumann, Isotope dilution mass spectrometry (IDMS) of the Elements, Mass Spectrom. Rev. 11 (1992) 41–67.

[14] W. Riepe, H. Kaiser, Massenspektrometrische Spurenanalyse von Calcium, Strontium und Barium in Natriumazid durch Isotopenverdünnungstechnik, Z. Anal. Chem. 223 (1966) 321–335.

[15] P. Klingbeil, J. Vogl, W. Pritzkow, G. Riebe, J. Müller, Comparative studies on the certification of reference materials by ICPMS and TIMS using isotope dilution procedures, Anal. Chem. 73 (2001) 1881–1888.

[16] M.J.T. Milton, J. Wang, High accuracy method for isotope dilution mass spectrometry with application to the measurement of carbon dioxide, Int. J. Mass Spectrom. 218 (2002) 63–73.

[17] J.R. de Laeter, J.K. Böhlke, P. De Bièvre, H. Hidaka, H.S. Peiser, K.J.R. Rosman, P.D.P. Taylor, Atomic weights of the elements: review 2000 (IUPAC Technical Report), Pure Appl. Chem. 75 (2003) 683–800.

[18] G. Audi, A.H. Wapstra, C. Thibault, The AME2003 atomic mass evaluation (II): Tables, graphs and references, Nucl. Phys. A 729 (2003) 337–676.

[19] G. Mana, O. Rienitz, A. Pramann, Measurement equations for the determination of the Si molar mass by isotope dilution mass spectrometry, Metrologia 47 (2010) 460–463.

[20] A. Montaser (Ed.), Inductively Coupled Plasma Mass Spectrometry, Wiley–VCH, New York, 1998.

[21] J. Vogl, Calibration Strategies and Quality Assurance, in: S.M. Nelms (Ed.), Inductively Coupled Plasma Mass Spectrometry Handbook, Blackwell Publishing Ltd., Oxford, 2005, pp. 146–181.

[22] E. Ponzevera, C.R. Quétel, M. Berglund, P.D.P. Taylor, P. Evans, R.D. Loss, G. Fortunato, Mass Discrimination during MC-ICP-MS isotopic ratio measurements: investigation by means of synthetic isotopic mixtures (IRMM-007 series) and application to the calibration of natural-like zinc materials (including IRMM-3702 and IRMM-651), J. Am. Soc. Mass Spectrom. 17 (2006) 1412–1427.

[23] M.E. Wieser, J.B. Schwieters, The development of multiple collector mass spectrometry for isotope ratio measurements, Int. J. Mass. Spectrom. 242 (2005) 97–115.

[24] S. Weyer, J.B. Schwieters, High precision Fe measurements with high mass resolution MC-ICPMS, Int. J. Mass. Spectrom. 226 (2003) 355–368.

[25] E. Engström, I. Rodushkin, D.C. Baxter, B. Öhlander, Chromatographic purification for the determination of dissolved silicon isotopic compositions in natural waters by high-resolution multicollector inductively coupled plasma mass spectrometry, Anal. Chem. 78 (2006) 250–257.

[26] S.H.J.M. van den Boorn, P.Z. Vroon, C.C. van Belle, B. van der Waagt, J. Schwieters, M.J. van Bergen, Determination of silicon isotope ratios in silicate materials by high-resolution MC-ICP-MS using a sodium hydroxide sample digestion method, J. Anal. Atom. Spectrom. 21 (2006) 734–742.

[27] BIPM, Evaluation of measurement data—guide to the expression of uncertainty in measurement, JCGM 100:2008.

[28] GUM-Workbench ™, Version 1.2.11.56 Win32© '96-'99 by Metrodata GmbH.

[29] I. Mills, T. Cvitaš, K. Homann, N. Kallay, K. Kuchitsu (Eds.), International Union of Pure and Applied Chemistry: Quantities, Units and Symbols in Physical Chemistry, Blackwell Science Ltd, Oxford, 1993.

[30] K. Fujii, A. Waseda, N. Kuramoto, S. Mizushima, P. Becker, H. Bettin, A. Nicolaus, U. Kuetgens, S. Valkiers, P. Taylor, P. De Bièvre, G. Mana, E. Massa, R. Matyi, E.G. Kessler, M. Hanke Jr., Present state of the Avogadro constant determination from silicon crystals with natural isotopic compositions, IEEE Trans. Instrum. Meas. 54 (2005) 854–859.

[31] P. Becker, H. Friedrich, K. Fujii, W. Giardini, G. Mana, A. Picard, H.-J. Pohl, H. Riemann, S. Valkiers, The Avogadro constant determination via enriched silicon-28, Meas. Sci. Technol. 20 (2009) 092002.

[32] B. Andreas, Y. Azuma, G. Bartl, P. Becker, H. Bettin, M. Borys, I. Busch, M. Gray, P. Fuchs, K. Fujii, H. Fujimoto, E. Kessler, M. Krumrey, U. Kuetgens, N. Kuramoto, G. Mana, P. Manson, E. Massa, S. Mizushima, A. Nicolaus, A. Picard, A. Pramann, O. Rienitz, D. Schiel, S. Valkiers, A. Waseda, An accurate determination of the Avogadro constant by counting the atoms in a ^{28}Si crystal, Phys. Rev. Lett. 106 (2011) 030801-1–0308014-0308014.